An anti-CTLA-4 heavy chain–only antibody with enhanced T_reg depletion shows excellent preclinical efficacy and safety profile

Xin Gan[a], Qianqian Shan[a], He Li[a], Rick Janssens[a,b], Yuqiang Shen[a], Yun He[a], Fei Chen[a], Rien van Haperen[a,b], Dubravka Drabek[a,b] 🄳, Jin Li[a], Yang Zhang[a] 🄳, Jiuqiao Zhao[a], Beibei Qin[a] 🄳, Ming-Jin Jheng[a], Victor Chen[a], Jingsong Wang[a], Yiping Rong[a], and Frank Grosveld[a,b,1]

The value of anti-CTLA-4 antibodies in cancer therapy is well established. However, the broad application of currently available anti-CTLA-4 therapeutic antibodies is hampered by their narrow therapeutic index. It is therefore challenging and attractive to develop the next generation of anti-CTLA-4 therapeutics with improved safety and efficacy. To this end, we generated fully human heavy chain–only antibodies (HCAbs) against CTLA-4. The hIgG1 Fc domain of the top candidate, HCAb 4003-1, was further engineered to enhance its regulatory T (T_reg) cell depletion effect and to decrease its half-life, resulting in HCAb 4003-2. We tested these HCAbs in in vitro and in vivo experiments in comparison with ipilimumab and other anti-CTLA4 antibodies. The results show that human HCAb 4003-2 binds human CTLA-4 with high affinity and potently blocks the binding of B7-1 (CD80) and B7-2 (CD86) to CTLA-4. The results also show efficient tumor penetration. HCAb 4003-2 exhibits enhanced antibody-dependent cellular cytotoxicity function, lower serum exposure, and more potent anti-tumor activity than ipilimumab in murine tumor models, which is partly driven by a substantial depletion of intratumoral T_regs. Importantly, the enhanced efficacy combined with the shorter serum half-life and less systemic drug exposure in vivo potentially provides an improved therapeutic window in cynomolgus monkeys and preliminary clinical applications. With its augmented efficacy via T_reg depletion and improved safety profile, HCAb 4003-2 is a promising candidate for the development of next generation anti-CTLA-4 therapy.

HCAb | anti-CTLA-4 Ab | ADCC killing | intratumoral T_reg depletion | anti-tumor efficacy

Advances in immunotherapy have transformed cancer treatment. Among the most prominent are checkpoint inhibitors (CPIs), which have now become part of standard-of-care regimens for an increasing number of cancers. The first CPI, the anti-CTLA-4 antibody ipilimumab, shows an ∼20% response rate and contributes to long-term survival even up to 10 y in some patients (1, 2). More recently, a low dosage of ipilimumab was applied in a combination therapy with anti-PD-1 antibody (3). However, ipilimumab characteristically induces immune-related adverse events (irAEs), which make long-term treatment with full benefits unsustainable. It would therefore be advantageous to obtain a higher therapeutic index by developing more efficacious anti-CTLA-4 therapeutics with fewer side effects.

CTLA-4 is constitutively expressed on regulatory T (T_reg) cells, while, after their induction, it is also expressed on activated T cells. It outcompetes CD28 to prevent it from binding to CD80 (B7-1) and CD86 (B7-2) and suppresses T cell activation (4–6), which is used by tumor cells to evade immune surveillance. Anti-CTLA-4 antibodies that block such negative regulation will promote systemic T cell activation and therefore sustain and prolong disease control. However, high systemic exposure to anti-CTLA-4 antibodies and sustained inhibition of CTLA-4 molecules in normal tissues may also induce undesired irAEs (7).

The most common irAEs are inflammatory in nature, for example, rash, colitis, or hepatitis, and may represent a breaking of tolerance to self-antigens (8, 9). A dose-dependent increase of irAEs was observed. The irAEs related to ipilimumab were dependent on both peak concentration and the area under the curve (AUC) of the drug, although the timing of irAE onset was highly variable and unpredictable.

It is still a debate whether it is better to block the negative regulation of CTLA-4 in T effector (T_eff) cells or to deplete CTLA-4⁺ T_reg cells in the tumor microenvironment (TME) to increase anti-tumor efficacy. Blocking CTLA-4 appears to mainly work at the priming stage to induce T cell activation (10–12). In addition to blocking CTLA-4 signaling, anti-CTLA-4 mAbs directly impact the CTLA-4^high CD4⁺Foxp3⁺ T_reg cell compartment, either by mediating depletion via antibody-dependent cellular cytotoxicity (ADCC) or by affecting their suppressive activity (13–16). Indeed, in cancer patients, FOXP3⁺

Significance

This article describes a fully human therapeutic heavy chain–only antibody for anti-tumor treatment. We show that this anti-CTLA-4 antibody, HCAb 4003-2, has advantageous properties and stimulates anti-tumor T cell activation in several ways: 1) It binds human CTLA4 with high affinity; 2) it effectively depletes tumor-resident regulatory T cells, leading to enhanced antibody-dependent cellular cytotoxicity (ADCC); 3) with its small size, it shows potent tumor penetration, thereby more widely exerting its effect on T cell activation; and 4) the enhanced efficacy combined with the shorter serum half-life and less systemic drug exposure in vivo potentially provides an improved therapeutic window in clinical applications.

T_{reg} cells migrate into the TME and suppress various types of effector lymphocytes, including $CD4^+$ Th cells and $CD8^+$ CTLs (17). In a preclinical study, a murine IgG2a anti-CTLA-4 mAb exhibited enhanced ADCC (eADCC)-dependent intratumor T_{reg} depletion and robust tumor control when compared to IgG2b and IgG1 murine anti-CTLA-4 mAbs (18). Tumor regression was shown to be associated with an increase in the intratumoral T_{eff} to T_{reg} cell ratio, due to an expansion of T_{eff} cells and selective depletion of T_{reg} cells (18, 19). Contrary to prior findings in a number of preclinical mouse models, it was observed that ipilimumab treatment resulted in an increased rather than reduced density of $Foxp3^+$ T_{reg} in tumors from melanoma, prostate, and bladder cancer patients (20). Thus, anti-CTLA-4 antibodies with eADCC and T_{reg} depletion may result in more potent and durable responses in cancer patients (21).

We aimed to develop an anti-CTLA-4 antibody with a shortened half-life and eADCC function, which would lower systemic exposure of anti-CTLA-4 antibodies and reduce the irAEs. However, it should not affect T_{reg} depletion or T cell activation in the priming stage. The eADCC function would help to deplete T_{reg} cells in the TME more effectively, thereby enhancing its antitumor efficacy. In contrast to camelid heavy chain–only CTLA-4 antibodies (WO2019233413), we developed fully human heavy chain–only antibodies (HCAbs) (22), which are natural, small, and stable antibodies first found in Camelids (23, 24). The antigen-binding domain of HCAbs is composed of only VH, and lacks light chains plus the CH1 domain of the heavy chain constant region. Single-domain antibodies have the advantage of being small, which potentially lowers their immunogenicity while achieving enhanced tumor penetration as suggested for llama VHH regions (25–27) and may even penetrate through the blood–brain barrier (28). Here we report an anti-CTLA-4 HCAb, 4003-2, with an engineered Fc region to simultaneously enhance its ADCC function and shorten its half-life. HCAb 4003-2 shows T_{reg} depletion in tumor tissues and favorable safety and efficacy in cynomolgus monkeys and a preliminary clinical study (29). Potentially, HCAb 4003-2 is an exciting next-generation anti-CTLA-4 antibody therapeutic candidate with impressive efficacy and reduced toxicity.

Results

Fully human anti-CTLA-4 HCAbs were generated from Harbour HCAb Mice, that have inactivated murine immunoglobulin loci and carry a human VH antibody locus (22, 30, 31). These antibodies therefore do not need additional humanization. Mice were immunized with human CTLA-4 recombinant protein (Fig. 1) and HCAbs isolated and screened using a rapid direct cloning approach (ref. 22 and Fig. 1), yielding a panel of potent anti-CTLA-4 HCAbs. The binding affinities and epitopes of HCAbs were evaluated both on human and cynomolgus monkey CTLA4 (*SI Appendix*, Table S1), and one of the top candidate clones, HCAb 4003-1, was further engineered with S239D and I332E (DE) mutations in the human IgG1 Fc constant domain to enhance its T_{reg} depletion effect and decrease its half-life in vivo (32), resulting in HCAb 4003-2. The engineered candidate HCAb 4003-2 was evaluated in in vitro T cell activation assays, in vitro and in vivo T_{reg} depletion assays, in vivo anti-tumor efficacy, safety studies, and in vivo pharmacokinetics (PK) analyses.

HCAb 4003-2 Induces a More Potent T Cell Activation When Compared to 4003-1 and Ipilimumab. T cell activation is a key activity induced by anti-CTLA-4 antibodies to modulate the
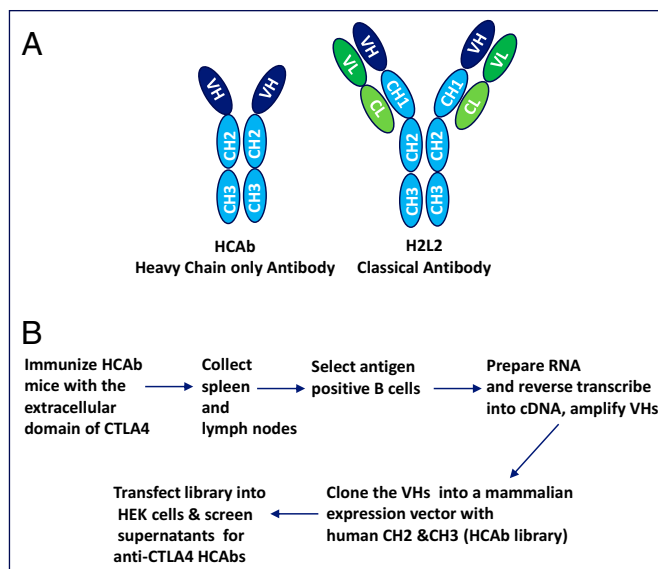

Fig. 1. Generation of anti-CTLA4 HCAbs. (*A*) The difference between heavy chain only antibodies lacking the CH1 constant domain and classical antibodies containing heavy and light chains. (*B*) The different steps to generate anti-CTLA4 HCAbs.

immune system. To test and compare the T cell activation potency of anti CTLA-4 antibodies, ipilimumab (see SI, ipilimumab analog in supplementary reagents), HCAb 4003-1, HCAb 4003-2 (Table S2, *SI Appendix*, Fig S1), BMS986218 (*SI Appendix*, Figs. S1 and S3), and Agen 1181 (*SI Appendix*, Figs. S2 and S3), IL-2 release was evaluated by enzyme-linked immunosorbent assay (ELISA) in human peripheral blood mononuclear cells (PBMCs) treated with staphylococcal enterotoxin B (SEB). HCAb 4003-2, HCAb 4003-1, and ipilimumab all induced IL-2 release in a dose-dependent manner (Fig. 2A and *SI Appendix*, Table S2). The maximal IL-2 release by HCAb 4003-1 was similar to ipilimumab, suggesting a similar T cell activation potency. The IL-2 release induced by HCAb 4003-2 was superior (more than fivefold) to that by either HCAb 4003-1 or ipilimumab.

To evaluate whether HCAb 4003-1 and 4003-2 would bind the same or a different epitope when compared to ipilimumab, the complex of human CTLA-4 and 4003-1 (VH) was crystallized and its structure determined at 2.38 Å (Protein Data Bank [PDB] code: 7DV4, not released yet), with HCAb 4003-1 and 4003-2 having an identical VH domain. The structures of CTLA-4/4003-1 (VH) and CTLA-4/ipilimumab (PDB code: 5TRU) were superimposed and compared using PyMOL by overlaying 4003-1 (VH) onto the heavy chain of ipilimumab (rmsd: 0.55 Å). Notably, the orientation of CTLA-4 in the CTLA-4/4003-1 (VH) complex (for details, see *SI Appendix*, Figs. S5–S7) was different from ipilimumab in complex with CTLA-4. The epitope recognized by 4003-1 (VH) is not the same but overlaps, to a large extent, those recognized by ipilimumab (Fig. 2B). Residues C50, A51, T53, Y54, M55, T61, and L63 of CTLA-4 were bound exclusively by 4003-1, and residues A2, M3, H4, L39, Q45, V46, K95, P102, P103, Y105, L106, G107, and I108 of CTLA-4 were bound exclusively by ipilimumab, while E33, R35, E48, E97, M99, Y100, and Y104 of CTLA-4 are recognized by both 4003-1 and ipilimumab. In total, HCAb 4003-1 interacts with 14 residues of CTLA-4 (*SI Appendix*, Table S14), while ipilimumab interacts with 20 residues.

To further evaluate whether the increased T cell activation capability of HCAb 4003-2 relative to ipilimumab was due to
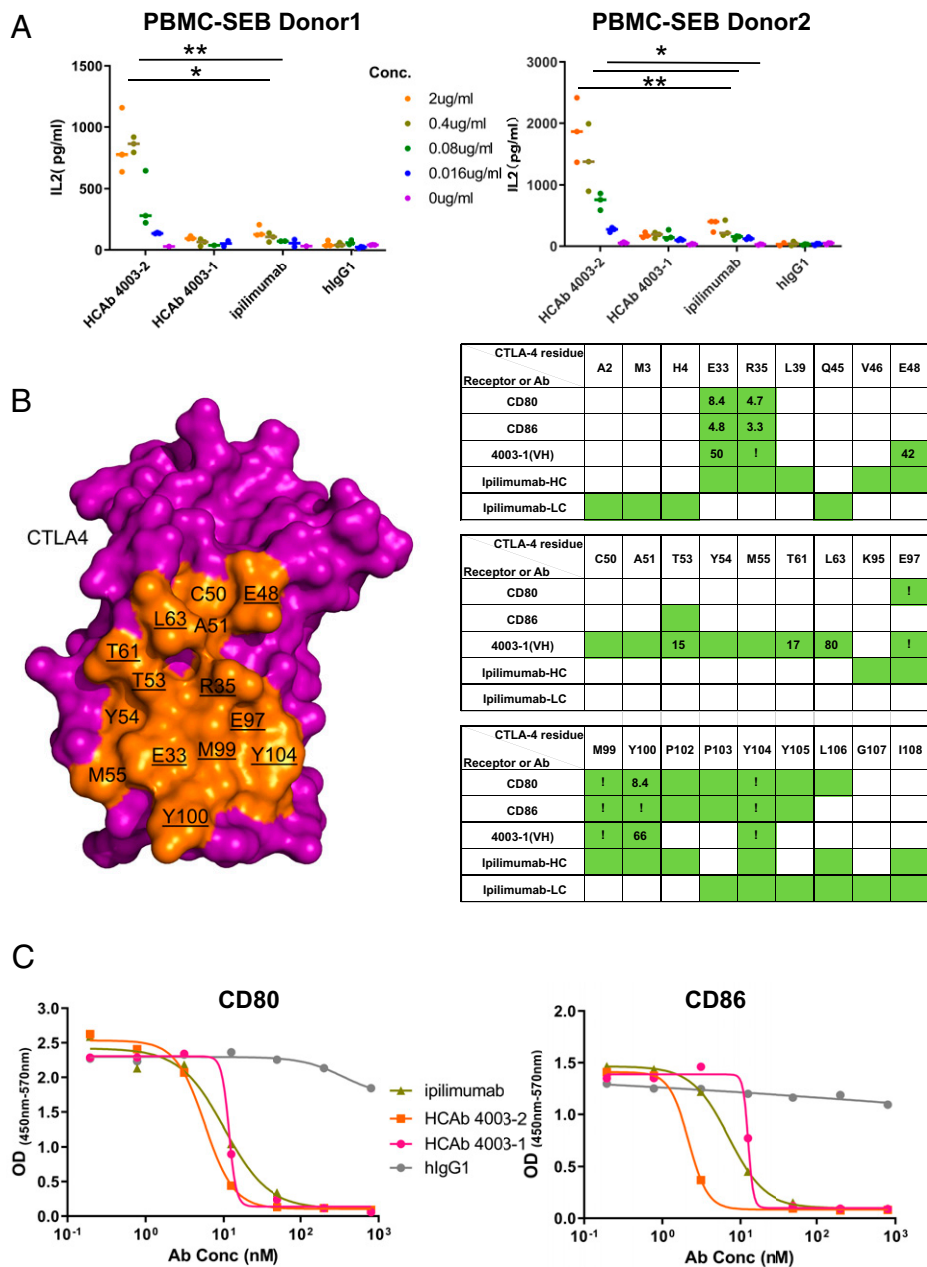
Fig. 2. PBMC-SEB assays and the binding epitope on CTLA-4 recognized by 4003-1 (VH). (*A*) HCAb 4003-2 induces high IL-2 release in human PBMC–SEB assay from two donors. The experiment was performed with triplicate samples, and the average ± SD is shown. *$P < 0.05$, **$P < 0.01$ by two-tailed unpaired Student's *t* test. (*B*). The surface of CTLA-4 is shown in purple, and the epitope is shown in orange. Individual residues are labeled in one-letter code. Key residues of the epitope are underlined. CTLA-4 residues involved in interaction with CD80, CD86, 4003-1(VH), and ipilimumab are shown. Residues are highlighted in green if they contact the binding partner as revealed by PyMOL. An exclamation mark (!) indicates that binding of the CTLA-4 mutant (mutated to alanine) to the binding partner was totally abolished as evidenced in an Octet assay, and the numbers show the fold changes of decrease in affinity. HC, heavy chain; LC, light chain. (*C*) Blocking of CTLA-4/B7.1 or CTLA/B 7.2 interaction by hIgG1, ipilimumab, and HCAb 4003-1 and 4003-2 by ELISA.

CTLA-4 residue / Receptor or Ab	A2	M3	H4	E33	R35	L39	Q45	V46	E48
CD80				8.4	4.7				
CD86				4.8	3.3				
4003-1(VH)				50	!				42
Ipilimumab-HC				■	■	■		■	
Ipilimumab-LC	■	■	■				■		

CTLA-4 residue / Receptor or Ab	C50	A51	T53	Y54	M55	T61	L63	K95	E97
CD80									!
CD86									
4003-1(VH)			15			17	80		!
Ipilimumab-HC								■	■
Ipilimumab-LC									

CTLA-4 residue / Receptor or Ab	M99	Y100	P102	P103	Y104	Y105	L106	G107	I108
CD80	!	8.4	■	■	!		■		
CD86	!	!	■	■	!				
4003-1(VH)	!	66			!				
Ipilimumab-HC	■		■				■	■	■
Ipilimumab-LC	■	■	■	■	■				■

blocking the interaction of CTLA4 with CD80 or CD86, we employed ELISA. The results showed that HCAb 4003-2 has similar blocking of the binding of CTLA-4 to CD80 or CD86 similar to HCAb 4003-1 and ipilimumab (Fig. 2*C*). We therefore determined whether the enhanced T cell activation capability of HCAb 4003-2, indicated by the increased IL-2 release, could be attributed to its enhanced activity and thereby release T cell suppression by T$_{reg}$ cells.

HCAb 4003-2 Enhances T$_{reg}$ Depletion In Vitro and In Vivo. T$_{reg}$ depletion is critical for the anti-tumor effect of anti-CTLA-4 antibodies in mice (19, 33–36), suggesting that the anti-CTLA-4 HCAb with an eADCC function may deplete T$_{reg}$

more efficiently. Hence, the ability of anti-CTLA-4 antibodies to induce NK cell–mediated lysis of human in vitro differentiated T$_{reg}$ cells or isolated pan-T cells (all CD3+ T cells) was assessed in an in vitro ADCC assay (Fig. 3*A*). HCAb 4003-2 showed, maximally, 60% lysis of in vitro differentiated T$_{reg}$ cells at 1 nMol concentration, which was much higher than seen with HCAb 4003-1 and ipilimumab, which showed, maximally, 10% lysis of T$_{reg}$ cells at a 10× higher concentration (Fig. 3*A*). The EC$_{50}$ of HCAb 4003-2 was about 100-fold more potent than ipilimumab. No significant lysis of isolated pan-T cells was observed with either HCAb 4003-1, HCAb 4003-2, or ipilimumab (Fig. 3*A*). To explain the differential lysis of human in vitro differentiated T$_{reg}$ and isolated pan-T cells, the surface

expression of CTLA-4 was determined by fluorescence-activated cell sorter (FACS). Approximately 21.4% and 29.2% of in vitro differentiated T_{reg} cells were Foxp3 and CTLA-4 double positive in two different donors, while CTLA-4 expression on isolated pan-T cells was almost undetectable in another two different donors (Fig. 3B). It indicates that T_{reg}-specific lysis was dependent on surface CTLA-4 expression.

To further explore the novel T_{reg} depletion mechanism of HCAb 4003-2, we evaluated the CD4, CD8, and T_{reg} cell population by FACS in tumor, spleen, and blood samples from mice inoculated with the murine colon carcinoma cell line MC38 (Gempharmatech). These mice had the human CTLA-4 gene knocked in, replacing the murine CTLA4 gene (37). They were treated with HCAb 4003-2 (G4 and G5) or ipilimumab (G2 and G3) versus a control anti PD1 antibody (hIgG1) (Fig. 3C), where 5.4 mg of HCAb 3002-2 is equimolar with 10 mg of ipilimumab or hIgG1. In tumor samples, a reduction of the percentage of T_{reg} cells in the CD4$^+$ population was observed in groups G4 or G5 treated with HCAb 4003-2 at 5.4 or 1.5 mg/kg, respectively (Fig. 3C and *SI Appendix*, Table S3). In spleen and blood samples, no notable change of the T_{reg} cells percentage in the CD4$^+$ cell population was observed in any

group (Fig. 3C and *SI Appendix*, Table S3). Hence, anti-CTLA-4 HCAb 4003-2 demonstrated enhanced T_{reg} depletion activity both in vitro and in vivo.

Next, we analyzed the kinetics of T_{reg} cell elimination by HCAb 4003-2 in mice. Animals were dosed, and samples were collected as scheduled in Fig. 3D. On day 2, about 63%, 30%, and 23% of CD4$^+$ T cells were CD25$^+$/Foxp3$^+$ tumor-resident T_{reg} cells in control, versus 5.4 or 1.0 mg/kg of 4003-2-treated mice (Fig. 3D and *SI Appendix*, Table S4). The percentages of tumor-resident T_{reg} cells were reduced by 52% and 63% compared to the human IgG1 group after one dosing of HCAb 4003-2 at 5.4 and 1.0 mg/kg, respectively (Fig. 3D and *SI Appendix*, Table S4).

On day 8, there were about 59% of tumor-resident CD25$^+$/Foxp3$^+$ T_{reg} cells in CD4$^+$ T cells in IgG1 dosed animals versus 23%, and 21% with three doses of control versus 1 and 5.4 mg/kg of 4003-2 (*SI Appendix*, Table S4). The tumor-resident T_{reg} cells were therefore reduced by about 51 to 62% compared to the human IgG1 control group after three doses of HCAb 4003-2 at 5.4 and 1.0 mg/kg (*SI Appendix*, Table S4). The percentages of T_{reg} cells in CD4$^+$ T cells were stable between day 2 and day 8 in control groups treated with 10 mg/kg
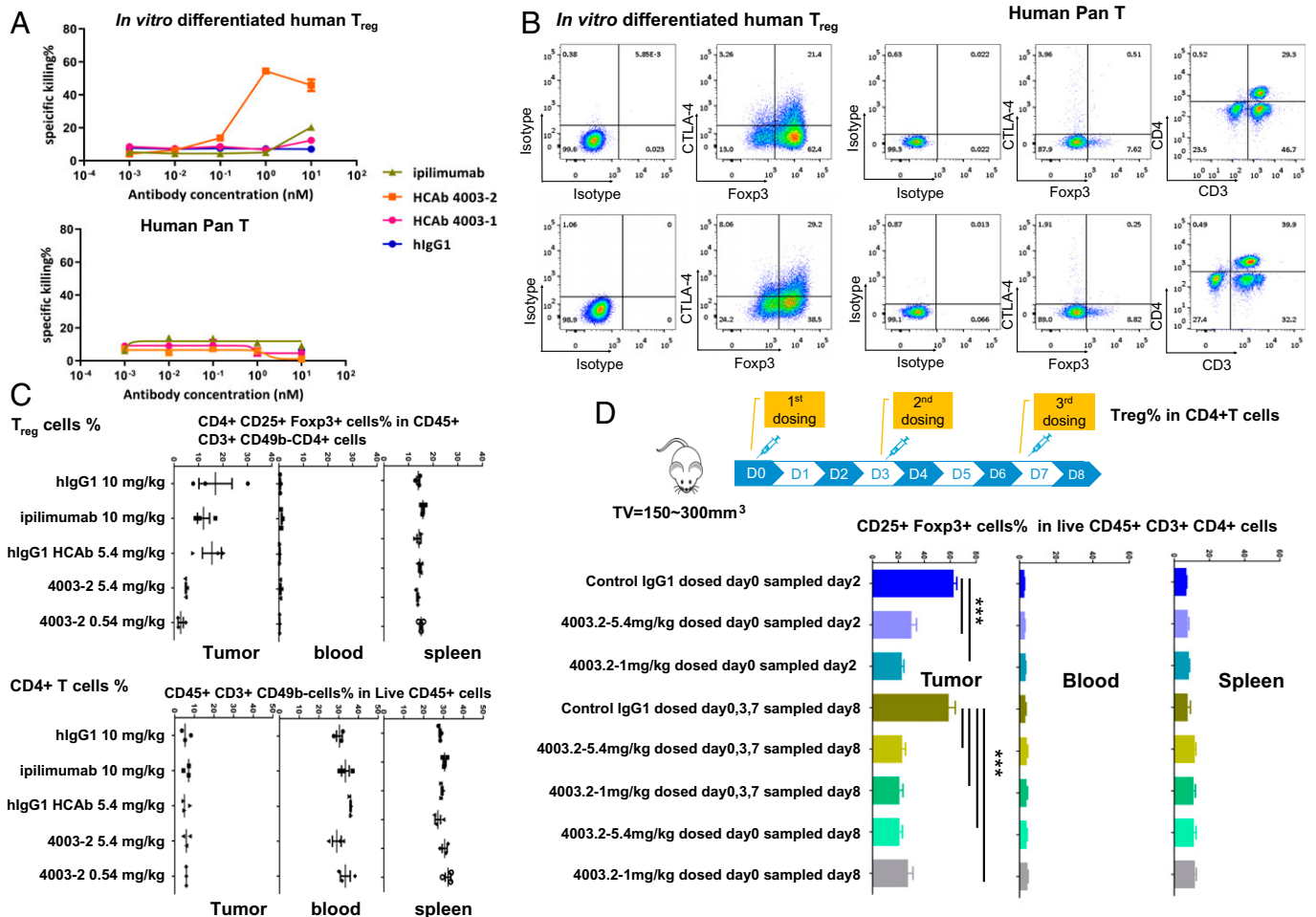

Fig. 3. In vitro activity of 4003-2 in an ADCC killing assay and TIL T_{reg} depletion of 4003-2 in MC38-bearing huCTLA-4 KI C57BL/6 mice. (A) HCAb 4003-2 induces potent cell lysis of in vitro differentiated human T_{reg} cells by fresh PBMC in ADCC killing assay, but does not result in cell lysis of primary human pan-T cells. (B) CTLA-4 expression is high on human T_{reg} and nondetectable on pan-T cells by flow cytometry. (C) T_{reg} cells are depleted in tumor but not in spleen or blood by 4003-2. G1, 10 mg/kg hIgG1; G2, 10 mg/kg ipilimumab; G3, 5.4 mg/kg hIgG1 HCAb; G4, 5.4 mg/kg 4003-2; G5: 1.5 mg/kg 4003-2. We do not think that the best reduction of the 0.54 mgs/mL 4003-2 is meaningful, as these are very low numbers and are caused by the virtual absence of T_{reg} cells in two of the mice. (D) The diagram shows the schedule of antibody dosing and sample collection. Percentages of T_{reg} population with different antibody treatments in mice tumor, spleen, and blood samples are shown. Data in bar graphs are presented as mean ± SD ***P < 0.001 by two-tailed unpaired Student's *t* test.

human IgG1. Interestingly, the level of T_{reg} depletion after 2 d of 5.4 or 1.0 mg/kg HCAb 4003-2 was similar. Next, we determined the minimal dosing frequency required for HCAb 4003-2 to maintain T_{reg} depletion. The percentages of tumor-resident T_{reg} cells in $CD4^+$ T cells were measured on day 8 in two groups: those dosed only on day 0 with 5.4 mg/kg HCAb 4003-2 and those dosed on both day 0 and day 3 with 5.4 mg/kg HCAb 4003-2. The percentages of tumor-resident T_{reg} cells were 21% and 27% of $CD4^+$ T cells in group single and double doses (*SI Appendix*, Table S4). The T_{reg} percentages of $CD4^+$ T cells in tumor tissues of these two groups were similar to that of the group with three dosages of 5.4 mg/kg (23%). We conclude that one dose of HCAb 4003-2 on day 0 was sufficient to achieve a sustainable T_{reg} depletion for at least 8 d in mice.

HCAb 4003-2 Exerts Potent Anti-tumor and Sustained Pharmacodynamical Effects In Vivo. To evaluate the associated anti-tumor activities of HCAb 4003-1 and 4003-2, a tumor growth inhibition (TGI) study was performed in human CTLA-4 knock-in (KI) C57BL/6 mice (33) at a dosing frequency of twice a week (BIW). Fig. 4A shows that the TGIs of ipilimumab at 1 mg/kg and 0.1 were 99% (*P* value ≤ 0.0001) and 59% (*P* value ≤ 0.05). The TGIs of HCAb 4003-1 at 0.54 and 0.054 mg/kg, that is, at a similar molarity as ipilimumab, were 100% (*P* value ≤ 0.0001) and 51% (*P* value ≤ 0.05) (*SI Appendix*, Fig. S4). The TGIs of HCAb 4003-2 at 0.54 and 0.054 mg/kg were 100% (*P* value ≤ 0.0001) and 95% (*P* value ≤ 0.0001) (Fig. 4A). The TGI of HCAb 4003-1 at 0.054 mg/kg was similar to that of ipilimumab at 0.1 mg/kg, but weaker than that of HCAb 4003-2 at 0.054 mg/kg. Therefore, HCAb 4003-2 showed better anti-tumor efficacy than both HCAb 4003-1 and ipilimumab.
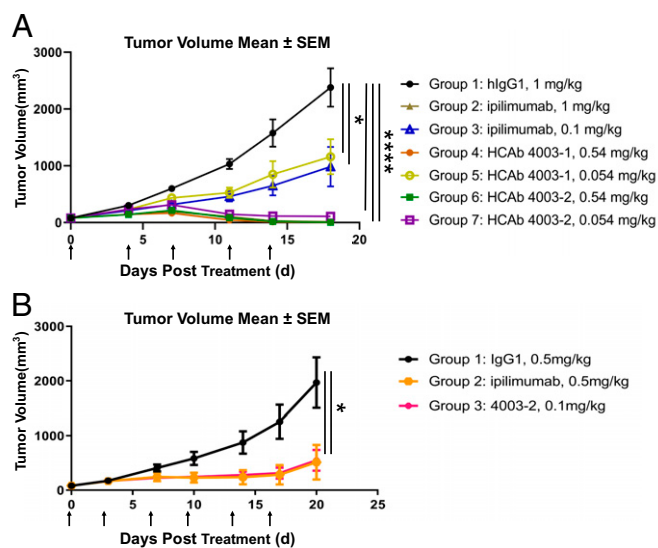
We next carried out a study with more-precise dose ranges of anti-CTLA-4 antibodies in the same mouse model. Fig. 4A shows no TGI of the human IgG1 HCAb-treated control group. The TGIs of ipilimumab at 0.5 and 0.2 mg/kg were 52% (*P* value ≤ 0.05) and 33% (Fig. 4A). The TGIs of HCAb 4003-2 at 0.1, 0.03, and 0.01 mg/kg were 91% (*P* value ≤ 0.001), 36%, and 18% (Fig. 4A). Thus the TGI of ipilimumab and HCAb 4003-2 was dose dependent. The TGI of HCAb 4003-2 at 0.03 mg/kg was similar to that of ipilimumab at 0.2 mg/kg. Therefore, HCAb 4003-2 achieved a similar anti-tumor efficacy at one-sixth the dose of ipilimumab (equivalent to a threefold molarity difference) and has a more potent anti-tumor efficacy than ipilimumab.

In another independent study performed in human CTLA-4 KI Balb/c mice bearing the *N*-nitroso-*N*-methylurethane-induced, undifferentiated colon carcinoma cell line CT26 (37), HCAb 4003-2 also showed a similar more potent anti-tumor efficacy than ipilimumab (Fig. 4B), probably caused by its enhanced T_{reg} depletion.

To evaluate the sustained T_{reg} depletion effect in MC38 tumor-bearing mice, we also reduced the dosing frequency of HCAb 4003-2 from BIW to once every 10 d in the MC38 mouse model. On day 23, the TGIs of groups treated with 0.1 mg/kg HCAb 4003-2 and 0.03 mg/kg HCAb 4003-2 were 99% and 57% (*SI Appendix*, Fig. S4). The anti-tumor efficacy of HCAb 4003-2 dosed every 10 d was as potent as that dosed BIW and was not affected by the reduced dosing frequency.

HCAb 4003-2 Has a Short Half-Life, High Tissue Penetration, and an Excellent Safety Profile. HCAb 4003-2 was designed not only to enhance T_{reg} depletion to achieve superior anti-tumor efficacy but also to shorten its half-life to potentially improve its safety profile. Hence, we evaluated the PK of HCAb 4003-2 in human CTLA-4 KI C57BL/6 mice. Fig. 5A shows that, after a single IV administration of HCAb 4003-2 at 5.4 mg/kg, the half-life and AUC of HCAb 4003-2 were much shorter and lower than those of ipilimumab and human IgG1 injected at a similar molarity; while the clearance of HCAb 4003-2 was much faster than ipilimumab (*SI Appendix*, Table S5). The difference was presumably due to the mutation in the Fc domain of HCAb 4003-2, since the PK profiles between HCAb 4003-1 and ipilimumab were not as pronounced (*SI Appendix*, Fig. S8 and Table S6). The anti-tumor efficacy of HCAb 4003-2 appears not to be affected by its shorter half-life (2.1 d), since it achieved similar tumor growth inhibition when dosed every 10 d compared to that dosed BIW.

We were also interested in the tumor penetration of HCAb because of its smaller size. To explore this, we measured the tumor/tissue penetration efficiency by radio-labeled HCAb 4003-2 in MC38 huCTLA-4 KI mice when compared to a classical monoclonal antibody (hIgG1; *SI Appendix*, Table S7). We dosed mice with 10 mg/kg HCAb 4003-2 or hIgG1 labeled by 200 µCi/kg [³H]. At 1 h or 24 h post dosing, most of radio signal was detected in mouse plasma (Table 1.). The peak of radio signal was detected at 1 h in most of the normal tissues, while it appeared at 24 h in the tumor (Fig. 5B). At 24 h, HCAb 4003-2 showed a very good antibody tissue distribution versus plasma of radio signals when compared to data obtained with classical H2L2 antibodies (see also ref. 38), with very good penetration of the HCAb in tumor/tissue (*SI Appendix*, Table S7). It was also consistent with the previous reports that smaller size is important, as observed with single-domain antibodies (15 kDa) from llama, which shows potent tissue distribution (25, 27). Thus, the higher tumor/tissue

Fig. 4. Potent in vivo efficacy of 4003-2 in MC38 bearing huCTLA-4 KI C57BL/6 mice. (*A*) Tumor volume change over time with different antibodies (ipilimumab at 0.5 and 0.2 mg/kg, and HCAb 4003-2 at 0.1, 0.03, and 0.01 mg/kg) dosed twice per week. Each group is randomized with nine mice. Tumor volume is presented as means ± SEM *P < 0.05, ****P < 0.001 by one-way ANOVA test. Treatment time is shown by arrows below the horizontal axis. (*B*) Potent in vivo efficacy of 4003-2 in CT26-bearing huCTLA-4 KI Balb/c mice. Tumor volume change is shown over time with different antibodies dosed twice per week. Each group is randomized with six mice. The data were expressed as mean ± SE (mean ± SEM). For comparison, an independent-samples *t* test was performed. Data were analyzed with SPSS. All tests were two-sided. *P* < 0.05 was considered to be statistically significant. GraphPad Prism was used.
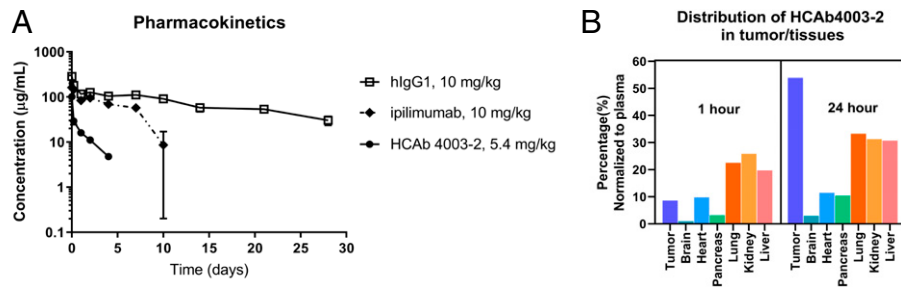
Fig. 5. PK of 4003-2 and its distribution in the mice tumor and organs at 1 and 24 h post dosing. (*A*) PK of hIgG1 (10 mg/kg), ipilimumab (10 mg/kg), and 4003-2 (5.4 mg/kg) following a single i.v. administration to female human CTLA-4 KI C57BL/6 mice (*n* = 3).(*B*) HCAb 4003-2 concentration in the tumor and organs at 1 and 24 h in huCTLA-4 KI mice bearing the MC38 tumor.

penetration of HCAb 4003-2 is, indeed, likely to contribute to its lower systemic exposure in serum and more efficacious antitumor activity.

To evaluate the safety profile of this fully human HCAb 4003-2, a single dose of 4003-2 at 30 mg/kg was intravenously (i.v.) administered in cynomolgus monkeys. No test article-related changes were noted in body weight, food consumption, body temperature, ECG, clinical chemistry, and macroscopic observation. Postdose findings included eyelid swelling in females and decreases in red blood cell count, hemoglobin, and hematocrit in males. Increases in white blood cell count, neutrophil percentage, lymphocyte percentage, and $CD3^+CD4^+$ cell percentage which may be related to the pharmacodynamic effect were noted in both sexes. Therefore, a single dose of 4003-2 at 30 mg/kg was well tolerated in cynomolgus monkeys.

Following the single-dose toxicity study of 4003-2 in cynomolgus monkeys, we performed an every-3-wk-dosing toxicity study at 3, 6, and 12 mg/kg by i.v. bolus, in a 3-mo period. In this study, the drug concentration of 4003-2 decreased quickly, showing low systemic drug exposure. However, increased populations of $Ki67^+CD4^+CD3^+$ T cells, $Ki67^+CD8^+CD3^+$ T cells, and absolute T cells were observed, indicating a desired pharmacodynamic effect. The only treatment-related clinical observation was an increased incidence of abnormal fecal findings, with a full recovery after cessation of 4003-2 administration. Minimal to slight inflammatory cell infiltrates in multiple organs were observed which represent the pharmacological effects of 4003-2. Thus, 4003-2 was well tolerated up to 6 mg/kg.

Discussion

Approximately 50 to 60% ipilimumab-treated patients experience systemic grade III to IV irAE, and a significant proportion of patients do not benefit from ipilimumab treatment. Improving drug efficacies and reducing side effects of anti-CTLA-4 antibodies is therefore still critical (10, 39). Here, we developed a next-generation anti-CTLA-4 fully human HCAb, HCAb 400-2, which has several key features: 1) an eADCC killing activity to tumor-infiltrating T_{reg} cells in vitro and in vivo, resulting in superior anti-tumor growth efficacy when compared to ipilimumab; 2) a long-lasting T_{reg} depletion and potent anti-tumor efficacy with reduced dose frequency and low drug exposure; 3) low systemic exposure resulting in a good safety profile; 4) binding affinities comparable to human and cynomolgus CTLA-4, making toxicity profiling from cynomolgus to human more predictable and translatable; and 5) fast and efficient penetration into tumor tissues, likely due to its smaller size.

Tumor rejection is associated with a depletion of tumor-infiltrating T_{reg} cells and a concomitant increase of the intratumoral T_{eff}/T_{reg} cell ratio. CTLA-4 was originally thought to play critical roles in the context of T cell receptor engagement (6), and antibody-mediated disruption of CTLA-4 blockade was well established (40). More recently, the importance of tumor-infiltrating T_{reg} depletion by anti-CTLA-4 antibodies in mouse studies was demonstrated (18, 34, 35). Anti-CTLA-4 mAbs with mouse IgG2a showed stronger T_{reg} depletion activity and more robust TGI relative to mouse IgG1 mAbs (18). However, it is still under debate whether ipilimumab shows a depletion of T_{reg} activity in patients, with reports that there is no notable T_{reg} depletion (20). First, the lack of T_{reg} depletion after ipilimumab treatment may, in part, be due to the absence of the CD16a-158V single-nucleotide polymorphism (SNP) variant in patients, since only effector cells with the CD16a-158V SNP variant show a good binding affinity to IgG1 antibodies (e.g., rituximab) and a notable ADCC activity (41, 42). Melanoma patients with the CD16a-158V SNP variant have a significantly improved overall survival versus those with the CD16a-158F (also named F176) SNP variant (35, 43, 44). Second, the suppressive effect cannot be mediated by the low level of fully competent NK cells in the TME to result in a constant ADCC killing of T_{reg} cells (35, 45). Our data also show that ipilimumab has a weak ADCC activity toward T_{reg} cells in vitro. Thus, anti-CTLA-4 therapy may be improved by engineering anti-CTLA-4 antibodies to enhance ADCC function to maximize the cytotoxicity of effector cells and fully utilize the limited number of effector cells in the TME. Third, the lack of detectable T_{reg} depletion in tumor tissues of patients after ipilimumab treatment may be due to TME heterogeneity (35).

HCAb 4003-2 was engineered to also have enhanced binding affinity to human CD16a (*SI Appendix,* Table S8). It had a twofold different affinity to the CD16a-158F and CD16a-158V SNP variants, and both are higher than that of ipilimumab (*SI Appendix,* Table S9). Presumably, HCAb 4003-2 will drive a potent and similar ADCC killing of tumor-resident T_{reg} cells in both CD16a-158F and CD16a-158V SNP.

HCAb 4003-2 showed a 100-fold more potent ADCC killing of human T_{reg} cells in vitro when compared to ipilimumab. The eADCC killing of T_{reg} cells by HCAb 4003-2 may directly contribute to the observed T cell activation, considering the comparable CTLA-4 blocking activity between HCAb 4003-2 and ipilimumab. Taken together, the enhanced T_{reg} depletion by HCAb 4003-2 reduced the T_{reg} suppression on effector T cells and synergized with CTLA-4 blocking activity to further boost T cell stimulation, leading to a robust anti-tumor efficacy in mouse studies.

Table 1. The [3H] 4003-2 concentration in tissues and ratio of tumor/tissue: plasma at 1 and 24 h in huCTLA-4 KI mice bearing the MC38 tumor

Time point	Tissue type	Tumor/tissue: plasma proportion	
		Value, %	Ratio to H2L2 antibody history data (35)
1 h	Tumor	8.61	ND
	Brain	0.96	2.73
	Heart	9.82	0.96
	Pancreas	3.23	0.50
	Lung	22.53	1.51
	Kidney	25.86	1.89
	Liver	19.74	1.63
	Plasma	100.00	1.00
24 h	Tumor	53.94	ND
	Brain	2.97	8.46
	Heart	11.48	1.13
	Pancreas	10.40	1.63
	Lung	33.27	2.23
	Kidney	31.29	2.28
	Liver	30.70	2.54
	Plasma	100	1.00

ND, Not Done.

This is corroborated by a significant difference in tumor-infiltrating T_{reg} depletion between HCAb 4003-2 and ipilimumab in our pharmacodynamics (PD) study. A stronger T_{reg} depletion was observed for HCAb 4003-2 compared to ipilimumab in mice tumors. Our findings indicate a correlation between T_{reg} depletion activity and anti-tumor efficacy of anti-CTLA-4 antibodies, consistent with previous reports (18–20, 43, 46). T_{reg} depletion was also supported by the enhanced binding affinity of HCAb 4003-2 and mouse CD16-2 when compared to 4003-1 (*SI Appendix*, Table S10).

Since CTLA-4 is also expressed on a proportion of $CD4^+FoxP3^-$ and $CD8^+$ T cells, we evaluated whether ADCC killing of HCAb 4003-2 is specific to T_{reg} cells only. The level of expression on Pan T cells, based on medium fluorescence intensity, was significantly lower than that seen on T_{reg} cells (Fig. 3*B*) (47, 48). This suggests that T_{reg} depletion enhancement may be a promising strategy for developing the next generation of immunotherapies, but more clinical data are needed to assess the potential risk of depleting other T_{eff} cells with CTLA-4 low expression.

Severe side effects (grades 3 to 4) of ipilimumab have been reported in about 25% of patients (49). The incidence of irAEs increased with an increase in systemic exposure to ipilimumab (1, 50), which may be reduced by lowering the systemic drug exposure (51). In a combination study of ipilimumab and nivolumab (anti PD-1 IgG4), the dosing of ipilimumab every 6 wk showed better safety profiles compared to dosing every 3 wk, in advanced hepatocellular carcinoma patients (52). Considering the T_{reg} depletion mechanism of HCAb 4003-2 and CTLA-4's function at the priming stage (10), we believe that long systemic exposure to HCAb 4003-2 is not required. The short half-life of HCAb 4003-2 was not due to its interaction with FcRn, since the binding affinities of 4003-1 and 4003-2 to mouse FcRn protein were similar (*SI Appendix*, Table S10), but was likely due to the S239D and I332E mutations in the Fc region, consistent with the reported reduced half-life of regular IgG1 antibodies with the DE mutation (53). The low drug exposure of HCAb 4003-2 was associated with a good safety profile. With either a single dose or repeated dose administration, HCAb 4003-2 showed good tolerability in cynomolgus monkeys , which indicates a promising safety profile in humans. Our preliminary phase1 data of HBM4003-2 show that it is well tolerated and appears to have a superior safety profile compared to the published ipilimumab clinical data. The current tolerable dose shows favorable PD regulation in patients, including Treg depletion (29).

To address whether low exposure impacts blocking activity and anti-tumor efficacy, we measured the anti-tumor efficacy of HCAb 4003-2 at a dosing frequency of every 10 d in a mouse model. It showed potent anti-tumor efficacy which was very similar to that observed with the BIW dosing. The reduction of exposure did not impact its anti-tumor activity, while the C_{max} was the same, suggesting that CTLA-4 blocking activity is important to prime T cell activation (10, 54), and synergizes with the T_{reg} depletion activity of HCAb 4003-2 to maintain T cell activation and an overall strong anti-tumor effect. This was further investigated by the PD study in mice. A single dose of HCAb 4003-2 on day 0 was sufficient to reduce the tumor-resident T_{reg} percentage in $CD4^+$ T cells for 48 h. No recovery was observed for tumor-infiltrating lymphocytes (TIL) T_{reg} in $CD4^+$ T cells for at least 6 d, even without any additional dosing. Interestingly, giving a dose of HCAb 4003-2 twice in the next 6 d gave no additional reduction of TIL T_{reg} percentage in $CD4^+$ T cells. The early time measurement of the kinetics of TIL T_{reg} depletion by anti-CTLA-4 antibodies in mice shows that the TIL T_{reg} depletion effect was potent and long lasting, as it was sustained for at least 8 d. The anti-tumor efficacy data demonstrate that the T_{reg} depletion activity of HCAb 4003-2 plays a critical role in anti-tumor immunity, in addition to its function at the priming stage. Thus HCAb 4003-2 stimulates anti-tumor T cell activation through two mechanisms, T_{reg} depletion and blocking the interaction between CTLA-4 and CD80(CD86), while its potential toxicity is reduced by preventing long-sustained exposure.

The different binding affinities of ipilimumab to human CTLA-4 versus cynomolgus CTLA-4 may explain why its severe toxicity in humans was not anticipated after the cynomolgus toxicology studies. More importantly, the high binding affinities of HCAb 4003-1, and its derivative HCAb 4003-2, to both human and cynomolgus CTLA-4 suggest that the toxicology study data in cynomolgus may be more predictive for the human safety profile.

HCAb 4003-2 is the first fully analyzed human HCAb, although camelid anti CTLA-4 HCAbs were reported previously. HCAb 4003-2 shows good distribution and penetration in the tumor and tissues. When compared to classical human monoclonal antibodies (see also ref. 38), the tumor/tissue to plasma proportion after HCAb 4003-2 dosing was much higher in several normal organs. This may be due to the exponential relationship that exists between molecular weight and biodistribution coefficient values (55), as the HCAb molecular weight (76 kDa) is half that of a classical H2L2 antibody (150 kDa). High penetration into tumor/tissue is essential for an anti-CTLA-4 Ab to block the target efficiently and thereby achieve high efficacy. A lower dose of HCAb 4003-2 with a higher tumor/tissue to plasma proportion, and a reduced systemic exposure, has the same efficacy as its H2L2 counterpart in the mouse tumor model.

Although we have demonstrated the marked efficacy and safety profiles of HCAb 4003-2 in animal models, its clinical efficacy and safety are still under investigation. It is, of course, not yet clear how the observations of HBM4003 on T_{reg} depletion and efficacy in mouse models translate to the human

cancer situation, considering the substantial differences in species-specific biology. Therefore, HBM4003 is being further validated in human clinical trials now. In a current phase 1 study with a small number of patients, the preliminary readouts suggest a long-lasting PD effect on T_{reg} depletion and a promising monotherapy efficacy signal in solid tumors which are in contrast to ipilimumab's published data.

Consistent with the preclinical murine efficacy and safety profiles of HCAb 4003-2, the preliminary data indicate that the T_{reg} depletion and low systemic exposure of HCAb 4003-2 are translated into the clinic. The preliminary clinical PD, efficacy, and safety data have been reported (2021 European Society for Medical Oncology meeting), and we look forward to strengthening these observations with more incoming human data. The clinical investigation of HCAb 4003-2 with anti-PD-1 antibodies as a combination therapy for oncology patients is also planned.

In conclusion, the nonclinical profile of HCAb 4003-2 generated from Harbour HCAb Mice appears sufficiently different from ipilimumab to warrant clinical development with the aim to demonstrate improved tumor inhibition. It represents a promising candidate of next-generation cancer immune therapeutics that could be applied broadly to large cancer patient populations, due to its excellent efficacy and safety profile, impressive biophysical properties, potential low immunogenicity, and high tumor penetration.

Materials and Methods

Study Design. In order to develop a next-generation therapeutic antibody targeting CTLA-4 with improved safety and better efficacy compared to ipilimumab, we generated an anti-CTLA-4 HCAb from Harbour HCAb Mice and engineered the Fc domain with the DE mutation (53) to shorten its half-life and enhance its binding to FcγRIIIA. The binding affinities of HCAbs 4003-1 (unmodified) and 4003-2 (DE modified) to CTLA-4 or Fc receptors were measured by Surface Plasmon Resonance. The in vitro function assays including the PBMC–SEB and ADCC assays were used to measure the activity of 4003-1, 4003-2, ipilimumab, BMS-986218, and Agen1181 (*SI Appendix*) for ligand blocking, T cell activation, ADCC-mediated T_{reg} depletion, etc. We further evaluated the anti-tumor efficacy and T_{reg} depletion of 4003-1, 4003-2 and ipilimumab in the MC38 murine human CTLA-4 KI syngeneic model. The PK profile of 4003-2 and ipilimumab was measured in C57BL/6 mice, and the safety profile of 4003-2 was investigated in cynomolgus monkeys.

Anti-CTLA-4 Antibody Generation. The antigen used for immunization was a his-tagged human CTLA-4/CD152 (AcroBiosystems CT4-H5229). Eight HCAb mice were immunized three times at 2-wk intervals with 20 μg of protein per mouse, and six were injected, additionally, five times with 44 μg of protein per mouse with 2-wk intervals between injections. Except for the first injections, where Stimune (Prionics; *SI Appendix, Supplementary Methods*) was used as an adjuvant, all boosts were done with the Ribi adjuvant (Sigma adjuvant system S6322-1VL; *SI Appendix, Supplementary Methods*). Mice with the highest titers were used as a source of lymphocytes for making the HCAb library. All animal experiments were approved by DEC Animal experimental comittee (NL).

Total RNA was prepared from antigen-specific B cells (*SI Appendix, Supplementary Methods* and Fig. 1). RNA was reverse transcribed to complementary DNA (cDNA) (*SI Appendix, Supplementary Methods*) for further transfection (*SI Appendix, Supplementary Methods*) in HEK cells. Ten days after cell incubation, all supernatants were screened with an ELISA assay (*SI Appendix, Supplementary Methods*). Two hundred microliters from each positive clone was used for an affinity screen on ForteBio Octet system (*SI Appendix, Supplementary Methods*).

Ipilimumab was synthesized according to the sequence released from IMGT or DrugBank. It was expressed from transfected HEK-293 cells. Antibodies were purified by protein A and determined to contain <0.5 endotoxin units per mg. The in-house purified antibody showed the same biochemical properties compared to commercially available Ipilimumab (*SI Appendix*).

Antibodies and Reagents. The control H2L2$_{TAA1}$ antibody was an anti-PD1 antibody (HBM9167; *SI Appendix, Table S7*). The secondary antibody Alexa Fluor 647 labeled goat anti-human IgG Fc (109-606-008) used in FACS was purchased from Jackson ImmunoResearch and Alexa Fluor 488 conjugated Goat anti-Human IgG (H+L). The other secondary antibody (A11013) was purchased from ThermoFisher; the recombinant CTLA-4 protein (CT4-H82F3) and its ligands, B7-1 (B71-H5259) and B7-2 (CD6-H5257), were all purchased from Acro Bio; the isotype antibody (C0001-4) used was purchased from Crown Bioscience; the PBMCs were isolated commercially and provided by Mt-Bio; the human naïve CD4$^+$ T Cell Isolation Kit II (130-094-131) and Pan T Cell Isolation Kit (130-096-535) were purchased from Mitenyi Biotec. For biolayer interferometry binding assays, wild-type CTLA-4 (CP33) was purchased from Novoprotein, and CD16a (V176) (CDA-H82E9) and CD16a (F176) (CDA-H82E8) were purchased from Acro Bio.

Cell Lines. Cell line MC38 (Gempharmatech) was cultured in RPMI-1640 Medium (Gibco, C11875500CP).

Measurement of Interaction between Ipilimumab, 4003-2, and CD16a. Binding of antibodies HCAb 4003-2 and ipilimumab with CD16a (V176) and CD16a (F176) was determined using Octet Red96e. CD16a (V176) or CD16a (F176) with an Avitag were loaded onto Streptavidin biosensors (ForteBio, 18-5019) to 0.25 nm to 0.3 nm. HCAb 4003-2 and ipilimumab of different concentrations (80, 40, 20, 10, 5, and 2.5 nM) were used as analytes. Double reference was applied.

Blocking ELISA. ELISA was used to assess the blocking activities of anti-CTLA-4 antibodies. Ninety-six-well plates (Corning, 9018) were first incubated with human B7-1 (Acro Bio, B71-H5259) (2 μg/mL) or human B7-2 protein (Acro Bio, CD6-H5257) (2 μg/mL) at 4 °C overnight. The plates were then washed with PBST (Medicago AB, 09-9410-100) and blocked with 1% bovine serum albumin (Thermo Scientific, 37525) for 2 h at room temperature. Plates were next incubated with anti-CTLA-4 antibodies from max dose 800 nM, 1:3 diluted to eight doses for 20 min at room temperature, followed with 0.25 μg/mL biotin-CTLA-4 (Acro Bio, CT4-H82F3) for 1 h at room temperature. Finally, plates were incubated with Precision Protein StrepTactin-HRP Conjugate (Bio Rad, 1610380) for 30 min and developed using TMB substrate (Biopanda, TMB-S003). The optical density of samples was detected at 450 and 570 nm.

Flow Cytometry Analysis of In Vitro Induced T_{reg} and Pan-T Cells. In vitro induced T_{reg} (iTreg) cells were differentiated from naive CD4$^+$ T cells and activated by precoated 5 μg/mL CD3 Monoclonal Antibody (OKT3) (eBioscience,16-0037-85) overnight at 4 °C. The coating plate first washed once with phosphate-buffered saline to remove unbound soluble CD3 antibodies, followed by adding resuspended naïve CD4$^+$ T cells at 3×10^5 cells per mL in culture medium (1,640 + 10% fetal bovine serum [FBS]) including 2 μg/mL CD28 Monoclonal Antibody (CD28.2) (eBioscience, 16-0289-85), 10 ng/mL IL-2 (Pepro-Tech, 200-02-B), and 20 ng/mL TGF-β (R&D, 240-B-002). Two hundred microliters of cells suspension was added per well in a 96-well plate (6×10^4 cells per well), and cultured at 37 °C for 4 d. Naive CD4$^+$ T cells were isolated from human PBMCs using the MACS human naive CD4 T-cell isolation kit II (Miltenyi Biotec, 130-094-131). Generated iTreg cells were confirmed using a staining antibody mixture against human CD4 (Biolegend, 317408), CD25 (Biolegend, 356108), CTLA-4 (Biolegend, 349908), and FoxP3 (Biolegend, 320208). Pan-T cells were isolated from human PBMCs using a Pan T Cell Isolation Kit (Meltenyi, 130-096-535). The obtained pan-T cells were confirmed using staining mixture against human CD3 (Biolegend, 300406) and CTLA-4 (Biolegend, 369611). The iTreg and pan-T cells were labeled with Calcein AM (Invitrogen, C34851) and used in the ADCC assay.

ADCC Assay. Five thousand Calcein AM-labeled iTregs and 500,000 allogeneic human PBMCs were plated in RPMI medium 1640 (Gibco, 11835030) containing 10% FBS (BI, 04-002-1A). A 10-fold serial dilution row of anti-CTLA4 antibodies was added at a starting concentration of 10 nM and incubated with the cells for 2 h at 37 °C. The plate was centrifuged at $300 \times g$ for 3 min before taking out 100 μL of supernatant for the Calcein AM release test. The ADCC assay of pan-T cells followed the same procedures, with the exception that the anti-CTLA4 antibodies were added at a starting concentration of 100 nM.

SEB-Activated Assay. Human PBMCs were freshly isolated from healthy deidentified human whole blood using Ficoll-Paque PLUS (GE, 17-1440-02) by gradient centrifugation; 1×10^5 PBMC cells were first incubated with anti-CTLA-4 antibodies (2 μg/mL, 0.4 μg/mL, 0.08 μg/mL, 0.016 μg/mL) for 30 min at 37 °C, then cultured with 400 ng/mL SEB (Superantigen SEB) (YiQin Biopharma) for 96 h at 37 °C in a 5% CO_2 incubator. IL-2 in the supernatant was measured using an ELISA kit (Thermo Fisher, 88-7025-88) in compliance with the manufacturer's instructions.

In Vivo Efficacy Study. In human CTLA-4 KI C57BL/6 mice, the exons expressing the extracellular domain of mouse CTLA-4 were replaced by the corresponding domains of human CTLA-4. Anti-CTLA-4 antibodies dosed twice per week were used to test the anti-tumor growth of Gemphamtech. MC38 cells (from Gemphamtech) were cultured in RPMI-1640 Medium (Gibco) with 10% FBS (Gibco), 100 U/mL penicillin, and 100 μg/mL Streptomycin (AMRESCO) and cultured at 37 °C in a 5% CO_2 atmosphere; 5×10^5 MC38 cells were collected, resuspended in DPBS, and transplanted in C57BL/6-hCTLA-4 animals. Animals were randomized ($n = 9$ per group) and treated with 0.5 mg/kg human IgG1, 0.1 mg/kg human IgG1 HCAb, 0.5 and 0.2 mg/kg ipilimumab, and 0.1, 0.03, and 0.01 mg/kg HCAb 4003-2 when the average tumor size reached 85 mm^3, with a dose administration on days 0, 3, 7, 10, 14, and 17. The various doses applied in the study were normalized to an equal molar concentration of antibody. Tumor size was measured by caliper twice weekly in two dimensions. The tumor volume was expressed in cubic millimeters using the formula

$$TV = (L \times W \times W)/2.$$

(TV, tumor volume; L, the long diameters of the tumor; and W, the short diameters of the tumor).

The key parameter, TGI %, was calculated using the formula

$$RTV_n = \frac{V_{nt}}{V_{n0}}$$
$$TGI = \left(1 - \frac{mean\ RTV_{treat}}{mean\ RTV_{vehicle}}\right) \times 100\%.$$

Anti-tumor growth of anti-CTLA-4 antibodies with a dosing schedule of every 10 d was also done with Gemphamtech. MC38-hPDL1 cells (from Gemphamtech) were cultured in 90% RPMI-1640 Medium (Gibco) with 10% FBS (Gibco), 100 U/mL penicillin, 100 μg/mL Streptomycin (AMRESCO), and 400 μg/mL G418 (Gibco, 10131-027) at 37 °C in a 5% CO_2 atmosphere; 1×10^6 MC38-hPDL1 cells were collected, resuspended in DPBS, and transplanted in C57BL/6-hPD1/hCTLA-4 animals. Animals were randomized ($n = 9$ per group) and treated with 1 mg/kg human IgG1, and 0.1 and 0.03 mg/kg HCAb 4003-2 when the average tumor size reached 91 mm^3, with dose administration on days 0, 10, and 20. Tumor size was measured as described above. The key parameter, TGI %, was calculated using the same formula as above.

In Vivo PD Study. The PD study was done at Chempartner. MC38 tumor cells (from Chempartner) were cultured as described above. Each huCTLA-4 KI C57BL/6 mouse was inoculated subcutaneously with 1×10^6 MC38 tumor cells for tumor development. Animals were randomized and treated with 10 mg/kg human IgG1, 10 mg/kg ipilimumab, 5.4 mg/kg hIgG1 HCAb, and 5.4 and 1.5 mg/kg 4003-2 when the average tumor size reached 373 mm^3. The various doses applied in the study were normalized to an equal molar concentration of antibody. Mice were treated with the second dose on day 3 and killed 24 h later to collect tumors, spleens, and blood samples for FACS analysis. The major endpoint was to determine the changes in the percentage of the different immune cell populations in tumor, blood, and spleen following antibody treatment in tumor-bearing mice.

For the in vivo T_{reg} depletion kinetic assay, MC38 tumor cells (from Chempartner) were cultured as described above. Each huCTLA-4 KI C57BL/6 mouse was inoculated subcutaneously with 1×10^6 MC38 tumor cells for tumor development. Animals were randomized and treated with human 5.4 mg/kg IgG1 HCAb, and 5.4 and 1.5 mg/kg 4003-2 when the average tumor size reached 155 mm^3. Mice were killed on scheduled days to collect tumors, spleens, and blood samples for FACS analysis. The major endpoint was to determine the changes in the percentage of the different immune cell populations in tumor, blood, and spleen following antibody treatment in tumor-bearing mice.

PK Study. Six female C57BL/6 mice of each group were treated with 10 mg/kg ipilimumab, 5.4 mg/kg 4003-2, or 10 mg/kg human IgG1 through an i.v. bolus dosing route. Sparse sampling was done of three mice serum samples at each time point. Serum samples were collected at predose, 5 min, 5 h, 24 h, and days 2, 4, 7, 10, 14, 21, and 28 after the single dose. Ipilimumab- and 4003-2-treated serum samples were measured by intact ELISA using biotinylated human CTLA-4 protein as the capture reagent (Acrobiosystems, CT4-H82E3) and goat anti-human IgG Fc polyclonal antibody (Jackson ImmunoResearch, 109-035-098) as the detection reagent. Human IgG1 treated serum samples were measured by total ELISA using Anti-human IgG F(c) as the capture reagent (Rockland Immunochemicals, 609-101-017) and goat anti-human IgG Fc polyclonal antibody (Jackson ImmunoResearch, 109-035-098) as the detection reagent.

Single-Dose Toxicity Study in Cynomolgus Monkeys. In this GLP complied single-dose toxicity study, cynomolgus monkeys, 1 per sex per group, were randomized to receive 4003-2 at 0 and 30 mg/kg as an i.v. bolus, and followed during a 2-wk observation period. The following parameters were assessed during the study: mortality/morbidity, clinical observations, body weight, food consumption, body temperature (rectal), ECG, hematology and coagulation, clinical chemistry, immune phenotyping, and gross anatomical examination at the termination.

Three-Month Repeated Dose Toxicity Study in Cynomolgus Monkeys. A total of 40 monkeys, 5 per sex per group, were randomized into four groups and dosed with 0 (vehicle), 3, 6, and 12 mg/kg 4003-2 by i.v. bolus every 3 wk for 3 mo (a total of six doses), followed by an 8-wk drug-free recovery period. Assessment of toxicity was based on mortality/morbidity, clinical observations, injection site skin irritation scoring, body weights, food consumption, ophthalmic observations, neurological examination, body temperature, blood pressure, respiration rate, pulse oximetry, ECG measurements, hematology, coagulation, clinical chemistry, and gross anatomic and histopathologic examinations. Blood samples were collected for toxicokinetic, immunogenicity, cytokine, T cell–dependent antibody response, immune phenotyping, and cardiac troponin evaluations. This study was carried out under GLP regulations.

Tissue Distribution Study. Human CTLA-4 KI mice bearing MC38 tumors (∼100 mm^3) were i.v. injected with 10 mg/200 μCi/kg [^{3}H] 4003-2 or H2L2TAA1 (*SI Appendix*, Table S7). After 1 and 24 h of dosing, mice were scarified. Tissues including blood, tumor, brain, lymph node (mesenteric), thymus, pancreas, skin, skeletal muscle, bone, bone marrow (femur), body fat, heart, lung, liver, kidney, spleen, bladder, uterus, ovary, and gastrointestinal wall were collected. After adding 1 N KOH and heating at 90 °C, the radioactivity of each sample was measured by liquid scintillation counter.

Statistics. For the in vivo efficacy study, the data of tumor volume and mouse body weight were expressed as a mean ± SE (mean ± SEM). One-way ANOVA with Dunnett post hoc test method was performed for comparison among three or more groups. All data were analyzed with GraphPad Prism version 7.0. $P < 0.05$ was considered statistically significant. $P < 0.01$ is noted as **, and $P < 0.001$ is noted as ***.

For the in vivo PD study and in vivo T_{reg} depletion kinetic assay, the cell populations between different groups were analyzed by one-way repeated measures ANOVA. Bonferroni's multiple comparisons test was used for the comparisons with vehicle group.

For the PK study, the PK parameters were calculated using noncompartmental analysis by the software WinNonlin 8.2.

Author affiliations: ^{a}Harbour BioMed, Shanghai 201203, China; and ^{b}Department of Cell Biology, Erasmus Medical Center, 3000 CA Rotterdam, The Netherlands

1. F. S. Hodi *et al.*, Improved survival with ipilimumab in patients with metastatic melanoma. *N. Engl. J. Med.* **363**, 711–723 (2010).
2. C. Robert *et al.*, Ipilimumab plus dacarbazine for previously untreated metastatic melanoma. *N. Engl. J. Med.* **364**, 2517–2526 (2011).
3. I. Pires da Silva *et al.*, Ipilimumab alone or ipilimumab plus anti-PD-1 therapy in patients with metastatic melanoma resistant to anti-PD-(L)1 monotherapy: A multicentre, retrospective, cohort study. *Lancet Oncol.* **22**, 836–847 (2021).
4. T. L. Walunas *et al.*, CTLA-4 can function as a negative regulator of T cell activation. *Immunity* **1**, 405–413 (1994).
5. M. F. Krummel, J. P. Allison, CD28 and CTLA-4 have opposing effects on the response of T cells to stimulation. *J. Exp. Med.* **182**, 459–465 (1995).
6. D. R. Leach, M. F. Krummel, J. P. Allison, Enhancement of antitumor immunity by CTLA-4 blockade. *Science* **271**, 1734–1736 (1996).
7. Center for Drug Evaluation and Research, Clinical pharmacology and biopharmaceutics review [Application Number:125377Orig1s000] . https://www.accessdata.fda.gov/drugsatfda_docs/nda/2011/125377Orig1s000ClinPharmR.pdf. Accessed 25 February 2011.
8. J. Weber, Review: Anti-CTLA-4 antibody ipilimumab: Case studies of clinical response and immune-related adverse events. *Oncologist* **12**, 864–872 (2007).
9. J. S. Weber, R. Dummer, V. de Pril, C. Lebbé, F. S. Hodi; MDX010-20 Investigators, Patterns of onset and resolution of immune-related adverse events of special interest with ipilimumab: Detailed safety analysis from a phase 3 trial in patients with advanced melanoma. *Cancer* **119**, 1675–1682 (2013).
10. B. T. Fife, J. A. Bluestone, Control of peripheral T-cell tolerance and autoimmunity via the CTLA-4 and PD-1 pathways. *Immunol. Rev.* **224**, 166–182 (2008).
11. E. I. Buchbinder, A. Desai, CTLA-4 and PD-1 pathways: Similarities, differences, and implications of their inhibition. *Am. J. Clin. Oncol.* **39**, 98–106 (2016).
12. J. A. Seidel, A. Otsuka, K. Kabashima, Anti-PD-1 and anti-CTLA-4 therapies in cancer: Mechanisms of action, efficacy, and limitations. *Front. Oncol.* **8**, 86 (2018).
13. S. Read, V. Malmström, F. Powrie, Cytotoxic T lymphocyte-associated antigen 4 plays an essential role in the function of CD25$^+$CD4$^+$ regulatory cells that control intestinal inflammation. *J. Exp. Med.* **192**, 295–302 (2000).
14. T. Takahashi *et al.*, Immunologic self-tolerance maintained by CD25$^+$CD4$^+$ regulatory T cells constitutively expressing cytotoxic T lymphocyte-associated antigen 4. *J. Exp. Med.* **192**, 303–310 (2000).
15. R. P. M. Sutmuller *et al.*, Synergism of cytotoxic T lymphocyte-associated antigen 4 blockade and depletion of CD25$^+$ regulatory T cells in antitumor therapy reveals alternative pathways for suppression of autoreactive cytotoxic T lymphocyte responses. *J. Exp. Med.* **194**, 823–832 (2001).
16. K. Wing *et al.*, CTLA-4 control over Foxp3+ regulatory T cell function. *Science* **322**, 271–275 (2008).
17. S. Spranger *et al.*, Up-regulation of PD-L1, IDO, and T$_{regs}$ in the melanoma tumor microenvironment is driven by CD8$^+$ T cells. *Sci. Transl. Med.* **5**, 200ra116 (2013).
18. M. J. Selby *et al.*, Anti-CTLA-4 antibodies of IgG2a isotype enhance antitumor activity through reduction of intratumoral regulatory T cells. *Cancer Immunol. Res.* **1**, 32–42 (2013).
19. T. R. Simpson *et al.*, Fc-dependent depletion of tumor-infiltrating regulatory T cells co-defines the efficacy of anti-CTLA-4 therapy against melanoma. *J. Exp. Med.* **210**, 1695–1710 (2013).
20. A. Sharma *et al.*, Anti-CTLA-4 immunotherapy does not deplete FOXP3$^+$ regulatory T cells (Tregs) in human cancers. *Clin. Cancer Res.* **25**, 1233–1238 (2019).
21. S. A. Quezada, K. S. Peggs, Lost in translation: Deciphering the mechanism of action of anti-human CTLA-4. *Clin. Cancer Res.* **25**, 1130–1132 (2019).
22. D. Drabek *et al.*, Expression cloning and production of human heavy-chain-only antibodies from murine transgenic plasma cells. *Front. Immunol.* **7**, 619 (2016).
23. C. Hamers-Casterman *et al.*, Naturally occurring antibodies devoid of light chains. *Nature* **363**, 446–448 (1993).
24. S. Muyldermans, C. Cambillau, L. Wyns, Recognition of antigens by single-domain antibody fragments: The superfluous luxury of paired domains. *Trends Biochem. Sci.* **26**, 230–235 (2001).
25. G. Lv *et al.*, PET imaging of tumor PD-L1 expression with a highly specific nonblocking single-domain antibody. *J. Nucl. Med.* **61**, 117–122 (2020).
26. P. Debie *et al.*, Size and affinity kinetics of nanobodies influence targeting and penetration of solid tumours. *J. Control. Release* **317**, 34–42 (2020).
27. D. Li *et al.*, Immuno-PET imaging of ^{89}Zr labeled anti-PD-L1 domain antibody. *Mol. Pharm.* **15**, 1674–1681 (2018).
28. X. Li *et al.*, The novel llama-human chimeric antibody has potent effect in lowering LDL-c levels in hPCSK9 transgenic rats. *Clin. Transl. Med.* **9**, 16 (2020).
29. S. Gu *et al.*, A phase I dose-escalation and expansion study of HBM4003, an anti-CTLA-4 heavy chain only monoclonal antibody, in patients with advanced solid tumors. *J. Clin. Oncol.* **40**, 2641 (2022).
30. D. Drabek, R. Janssens, R. van Haperen, F. Grosveld, "A transgenic heavy chain IgG mouse platform as a source of high affinity fully human single-domain antibodies for therapeutic applications" in *Single-Domain Antibodies: Methods and Protocols*, G. Husack, K. A. Henry, Eds. (Springer, 2022), pp. 121–141.
31. B. J. Laventie *et al.*, Heavy chain-only antibodies and tetravalent bispecific antibody neutralizing *Staphylococcus aureus* leukotoxins. *Proc. Natl. Acad. Sci. U.S.A.* **108**, 16404–16409 (2011).
32. G. A. Lazar *et al.*, Engineered antibody Fc variants with enhanced effector function. *Proc. Natl. Acad. Sci. U.S.A.* **103**, 4005–4010 (2006).
33. K. D. Lute *et al.*, Human *CTLA4* knock-in mice unravel the quantitative link between tumor immunity and autoimmunity induced by anti-CTLA-4 antibodies. *Blood* **106**, 3127–3133 (2005).
34. J. R. Ingram *et al.*, Anti-CTLA-4 therapy requires an Fc domain for efficacy. *Proc. Natl. Acad. Sci. U.S.A.* **115**, 3912–3917 (2018).
35. F. Arce Vargas *et al.*; TRACERx Melanoma; TRACERx Renal; TRACERx Lung consortia, Fc effector function contributes to the activity of human anti-CTLA-4 antibodies. *Cancer Cell* **33**, 649–663.e4 (2018).
36. D. Ha *et al.*, Differential control of human Treg and effector T cells in tumor immunity by Fc-engineered anti-CTLA-4 antibody. *Proc. Natl. Acad. Sci. U.S.A.* **116**, 609–618 (2019).
37. J. C. Castle *et al.*, Immunomic, genomic and transcriptomic characterization of CT26 colorectal carcinoma. *BMC Genomics* **15**, 190 (2014).
38. D. K. Shah, A. M. Betts, Antibody biodistribution coefficients: Inferring tissue concentrations of monoclonal antibodies based on the plasma concentrations in several preclinical species and human. *MAbs* **5**, 297–305 (2013).
39. A. Bertrand, M. Kostine, T. Barnetche, M. E. Truchetet, T. Schaeverbeke, Immune related adverse events associated with anti-CTLA-4 antibodies: Systematic review and meta-analysis. *BMC Med.* **13**, 211 (2015).
40. A. A. Tarhini, J. M. Kirkwood, CTLA-4-blocking immunotherapy with ipilimumab for advanced melanoma. *Oncology (Williston Park)* **24**, 1302, 1304 (2010).
41. S. Dall'Ozzo *et al.*, Rituximab-dependent cytotoxicity by natural killer cells: Influence of FCGR3A polymorphism on the concentration-effect relationship. *Cancer Res.* **64**, 4664–4669 (2004).
42. B. Burkhardt *et al.*, Impact of Fc gamma-receptor polymorphisms on the response to rituximab treatment in children and adolescents with mature B cell lymphoma/leukemia. *Ann. Hematol.* **95**, 1503–1512 (2016).
43. A. Snyder *et al.*, Genetic basis for clinical response to CTLA-4 blockade in melanoma. *N. Engl. J. Med.* **371**, 2189–2199 (2014).
44. E. M. Van Allen *et al.*, Genomic correlates of response to CTLA-4 blockade in metastatic melanoma. *Science* **350**, 207–211 (2015).
45. M. Vitale, C. Cantoni, G. Pietra, M. C. Mingari, L. Moretta, Effect of tumor cells and tumor microenvironment on NK-cell function. *Eur. J. Immunol.* **44**, 1582–1592 (2014).
46. Y. Bulliard *et al.*, Activating Fc γ receptors contribute to the antitumor activities of immunoregulatory receptor-targeting antibodies. *J. Exp. Med.* **210**, 1685–1693 (2013).
47. K. Shitara, H. Nishikawa, Regulatory T cells: A potential target in cancer immunotherapy. *Ann. N. Y. Acad. Sci.* **1417**, 104–115 (2018).
48. T. Matoba *et al.*, Regulatory T cells expressing abundant CTLA-4 on the cell surface with a proliferative gene profile are key features of human head and neck cancer. *Int. J. Cancer* **144**, 2811–2822 (2019).
49. K. C. Kähler, A. Hauschild, Treatment and side effect management of CTLA-4 antibody therapy in metastatic melanoma. *J. Dtsch. Dermatol. Ges.* **9**, 277–286 (2011).
50. J. D. Wolchok *et al.*, Ipilimumab monotherapy in patients with pretreated advanced melanoma: A randomised, double-blind, multicentre, phase 2, dose-ranging study. *Lancet Oncol.* **11**, 155–164 (2010).
51. Y. Feng *et al.*, Exposure-response relationships of the efficacy and safety of ipilimumab in patients with advanced melanoma. *Clin. Cancer Res.* **19**, 3977–3986 (2013).
52. A. B. El-Khoueiry *et al.*, Nivolumab in patients with advanced hepatocellular carcinoma (CheckMate 040): An open-label, non-comparative, phase 1/2 dose escalation and expansion trial. *Lancet* **389**, 2492–2502 (2017).
53. Y. T. Tai *et al.*, Potent in vitro and in vivo activity of an Fc-engineered humanized anti-HM1.24 antibody against multiple myeloma via augmented effector function. *Blood* **119**, 2074–2082 (2012).
54. M. K. Callahan, J. D. Wolchok, At the bedside: CTLA-4- and PD-1-blocking antibodies in cancer immunotherapy. *J. Leukoc. Biol.* **94**, 41–53 (2013).
55. Z. Li *et al.*, Influence of molecular size on tissue distribution of antibody fragments. *MAbs* **8**, 113–119 (2016).
56. X. Gan *et al.*, An anti-CTLA-4 heavy chain-only antibody with enhanced T$_{reg}$ depletion shows excellent preclinical efficacy and safety profile. Protein Data Bank. https://www.rcsb.org/structure/7DV4. Deposited 12 January 2022.